The Carbapenemase BKC-1 from *Klebsiella pneumoniae* Is Adapted for Translocation by Both the Tat and Sec Translocons

Manasa Bharathwaj,ᵃ Chaille T. Webb,ᵃ Grishma Vadlamani,ᵃ,ᵇ ⓘ Christopher J. Stubenrauch,ᵃ Tracy Palmer,ᶜ ⓘ Trevor Lithgowᵃ

ᵃInfection & Immunity Program, Biomedicine Discovery Institute and Department of Microbiology, Monash University, Melbourne, Victoria, Australia
ᵇThe University of Western Australia, School of Molecular Sciences & The ARC Centre of Excellence in Plant Energy Biology, Crawley, Western Australia, Australia
ᶜMicrobes in Health and Disease, Newcastle University Biosciences Institute, Newcastle University, Newcastle upon Tyne, United Kingdom

ABSTRACT The cell envelope of Gram-negative bacteria consists of two membranes surrounding the periplasm and peptidoglycan layer. β-Lactam antibiotics target the periplasmic penicillin-binding proteins that synthesize peptidoglycan, resulting in cell death. The primary means by which bacterial species resist the effects of β-lactam drugs is to populate the periplasmic space with β-lactamases. Resistance to β-lactam drugs is spread by lateral transfer of genes encoding β-lactamases from one species of bacteria to another. However, the resistance phenotype depends in turn on these "alien" protein sequences being recognized and exported across the cytoplasmic membrane by either the Sec or Tat protein translocation machinery of the new bacterial host. Here, we examine BKC-1, a carbapenemase from an unknown bacterial source that has been identified in a single clinical isolate of *Klebsiella pneumoniae*. BKC-1 was shown to be located in the periplasm, and functional in both *K. pneumoniae* and *Escherichia coli*. Sequence analysis revealed the presence of an unusual signal peptide with a twin arginine motif and a duplicated hydrophobic region. Biochemical assays showed this signal peptide directs BKC-1 for translocation by both Sec and Tat translocons. This is one of the few descriptions of a periplasmic protein that is functionally translocated by both export pathways in the same organism, and we suggest it represents a snapshot of evolution for a β-lactamase adapting to functionality in a new host.

IMPORTANCE Bacteria can readily acquire plasmids via lateral gene transfer (LGT). These plasmids can carry genes for virulence and antimicrobial resistance (AMR). Of growing concern are LGT events that spread β-lactamases, particularly carbapenemases, and it is important to understand what limits this spread. This study provides insight into the sequence features of BKC-1 that exemplify the limitations on the successful biogenesis of β-lactamases, which is one factor limiting the spread of AMR phenotypes by LGT. With a very simple evolutionary adaptation, BKC-1 could become a more effective carbapenemase, underscoring the need to understand the evolution, adaptability, and functional assessment of newly reported β-lactamases rapidly and thoroughly.

KEYWORDS β-lactamase, antimicrobial resistance, periplasm, signal peptide, Tat pathway, beta-lactamases, evolution, protein secretion

The adaptation of a bacterial species to a new niche can be promoted by the acquisition of additional genes by lateral gene transfer (LGT), but this requires that the newly acquired proteins are translated (1), localized (2), and folded into functional forms (3) to deliver the appropriate phenotype (4–7). Antimicrobial resistance (AMR) is such a phenotype and has become of grave concern for human health globally (8, 9). The enzymes that play a key role in the generation of AMR phenotypes in many bacteria are β-lactamases, providing resistance to β-lactam antibiotics. These enzymes are

typically active in the periplasm, where they hydrolyze the β-lactam ring of the drug, rendering it inactive (10, 11). Carbapenemases are a subset of β-lactamases effective against the carbapenem class of β-lactam antibiotics used to treat multidrug-resistant bacterial infections (12, 13). In addition to an extended-spectrum β-lactamase (ESBL) resistant phenotype, carbapenemases thereby provide a carbapenem-resistant pheno-type, and the widespread use of carbapenems has increased the prevalence of carba-penem-resistant *Enterobacteriaceae* (CRE) (12, 14, 15). There are two prominent types of carbapenemases: (i) the metallo-β-lactamases that require one or more zinc atoms to be coordinated in their active site (e.g., NDM-1), and (ii) the *K. pneumoniae* carbape-nemases that are not metalloenzymes but instead are serine β-lactamases (16). First described in 2001 (17), the most prominent is "<u>K</u>lebsiella <u>p</u>neumoniae <u>c</u>arbapenemase 2" or KPC-2 (encoded by bla_{KPC-2}) and the related variants are the major contributors to widespread CRE phenotypes (14, 18, 19). Genes such as these are found on mobile genetic elements, particularly plasmids, meaning that these genes are readily transmis-sible (16, 20–23).

To confer an AMR phenotype to the host species, β-lactamases acquired by LGT need to be present at sufficiently high steady-state levels, with this level dependent on the compound efficiency of protein synthesis, protein transport pathways, and protein folding. Thus, the phenotype demands efficiency of host cell processes despite that the "alien" protein from an LGT event did not coevolve with the host cell factors medi-ating these pathways. For example, there is a global distribution of the CTX-M family of β-lactamases in *E. coli* (24, 25), *K. pneumoniae* (26, 27), other *Enterobacteriaceae* (28, 29), and *Pseudomonas aeruginosa* (30, 31), implying that all of the species acquiring these genes are capable of efficiently translating the polypeptide through what might be nonoptimal codon bias, transporting it across the inner membrane via protein translocases that must recognize its signal peptide, and folding the CTX-M protein so that the functional form populates the periplasm. Studies directed at the CTX-M β-lac-tamases show that this requires the translocation of the nascent polypeptide across the inner membrane in an unfolded state, followed by protein folding reactions in the periplasm to generate the enzymatically active β-lactamase (32–34).

Most of the proteins that function in the periplasm are translocated across the inner membrane by the general secretory (Sec) pathway as linear polypeptide chains, and their folding in the periplasm is facilitated by a specific set of chaperones (35–38). In order to engage the Sec translocon, protein substrates possess an N-terminal signal peptide of about 17 to 24 amino acids in length, comprising a positively charged n-region, a highly hydrophobic h-region, and a polar c-region that includes the cleavage site for signal peptidase (39, 40). Given that the first serine β-lactamases evolved from penicillin binding proteins (41, 42), which utilize the Sec pathway for their translocation to the periplasm (43), it was assumed that these enzymes would also translocate via Sec. This assumption proved to be valid for most β-lactamases, including TEM-1, CTX-M-14, and AmpC, each of which have been widely distributed among drug-resistant *Enterobactericeae* (29, 44–47).

Given this paradigm, it was curious to see that a small cohort of chromosomally encoded serine β-lactamases, such as L2 from *Stenotrophomonas maltophilia* and BlaC from *Mycobacterium tuberculosis*, are not transported by the Sec translocon, but instead utilize the twin arginine translocase (Tat) machinery for translocation across the inner membrane (47, 48). This means that these few β-lactamases use an alternate pathway where they are first folded in the cytoplasm and only thereafter translocated as fully functional enzymes (47).

Substrate proteins that engage the Tat machinery possess an N-terminal signal pep-tide that is usually between 27 and 35 amino acids in length and that contains both Tat-targeting and Sec-avoidance features to ensure the exclusivity that is known to exist for these protein translocation pathways (49, 50). The major Tat recognition fea-ture is a pair of almost invariant arginine residues in the signal peptide n-region, found as part of the SRRXFL motif (49, 51). A combination of an h-region that is only

moderately hydrophobic, coupled with the presence of one or more positively charged residues in either the c-region or at the N terminus of the mature protein, serve as Sec avoidance elements (52–55). Thus, signal peptides have evolved to target their passenger proteins strictly to either the Tat or Sec machinery. For protein substrates acquired through LGT, this also matters in terms of the folding assistance they will be provided in the new host cell; intrinsic sequence and structural features that require folding by the chaperones in the periplasm posttranslocation (35, 36, 39) will only be satisfied if the protein is translocated in an unfolded state by the Sec translocon. Conversely, intrinsic sequence and structural features that require folding in the cytoplasm prior to translocation will only be satisfied if the protein is translocated in a folded state by the Tat translocon (56, 57). While recent studies suggest there is some leeway for overlapping features that define Sec or Tat signal peptides (53, 55), with the exception of the Sec-dependent lipase in *Bacillus subtilis* (58), which can overflow into the Tat pathway upon multicopy overproduction, there is very limited evidence that a single protein is capable of using both translocons in the same organism.

Initial studies on the signal peptides of *β*-lactamases revealed three putative Tat-transported enzymes: BKC-1 and GPC-1, first identified in clinical isolates of *K. pneumoniae* and *P. aeruginosa,* respectively (59–61), as well as PAD-1 from the soil bacterium *Paramesorhizobium desertii* (60). Here, we show that these three proteins represent an isolated subfamily of *β*-lactamases with carbapenemase activity. Furthermore, through the production of BKC-1 in a model strain of *E. coli* with or without a functional Tat system, we show that while a subpopulation of protein molecules are translocated by the Sec pathway, the rest are translocated via Tat translocon. Therefore, mounting a carbapenem-resistant phenotype depends on the presence of the Tat machinery to provide sufficient translocation of BKC-1 into the periplasm.

RESULTS

Equivalent plasmids carry *bla*$_{BKC-1}$ and *bla*$_{KPC-2}$. The plasmid p60136 harboring *bla*$_{BKC-1}$ was identified in a carbapenem-resistant *Klebsiella* isolate (59). Gene signatures, including the transposable element IS*Kpn23* (Fig. 1A), were suggestive of a gene transposition from another species via LGT. Sequence analyses revealed that p60136 is related to the globally disseminated pB29 (GenBank accession MK330869) and pKPC05 (GenBank accession MK330868) plasmids. However, rather than *bla*$_{BKC-1}$, these other two IncQ plasmids carry *bla*$_{KPC-2}$ flanked by elements from the transposon Tn*4401*, the transposase (*tnpA*) from IS*Kpn6* and the *tnpR*-encoded resolvase. Apart from these transposon elements that are characteristic of *bla*$_{KPC-2}$-harboring plasmids (62), the three plasmids have a high degree of sequence identity, including across the replication genes (Fig. 1A).

We sought to understand the overall sequence relationships between BKC-1 and other *β*-lactamases that have been identified globally. Using a 40% sequence identity cutoff as an indicator of diverse *β*-lactamases, sequences were extracted from BLDB (Beta-lactamase database) (63) and the top 200 hits were subsequently analyzed using iTOL (64) (Fig. 1B). Molecular phylogeny analysis in this global context demonstrated that BKC-1 is most closely related to GPC-1 from *P. aeruginosa* (61), and these two in turn are related to PAD-1 from the soil bacterium *P. desertii* (60). These proteins have a sequence identity of 66% (Fig. 1B), but no other closely related proteins are present in the BLDB.

Targeting and subcellular localization of BKC-1. The vast majority of bacterial signal peptides are 20 to 30 amino acids long (65). However, initial sequence analysis revealed an unexpected feature in the N-terminal region of nascent BKC-1, where an unusually long, 46-residue signal peptide that included a twin arginine motif (SRRQAI) and a putative cleavage site after Ala46 was present (Fig. 2A). A multiple sequence alignment of BKC-1 from *K. pneumoniae* with GPC-1 from *P. aeruginosa* and PAD-1 from *P. desertii* showed that a 16-residue duplication in the h-region of the signal peptide of BKC-1 is responsible for its increased length (Fig. 2B; Fig. S1 in the supplemental material).

To investigate the biochemical impact of these signal sequence features in BKC-1, we used the well-characterized *E. coli* model system to study its targeting and
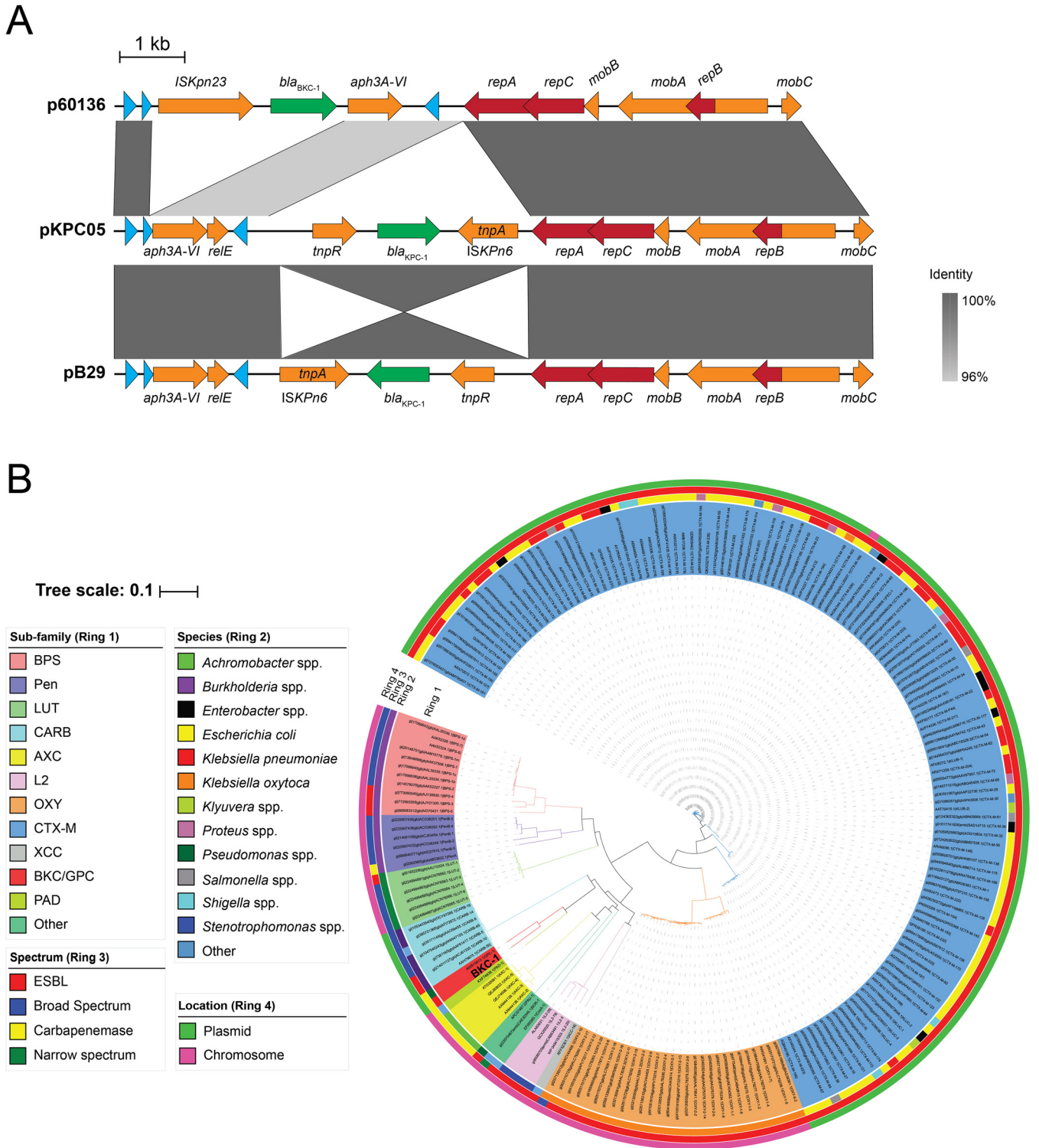
FIG 1 Comparison of the genetic environment of BKC-1. (A) The bla_{BKC-1} gene is carried on an RSF1010 plasmid, p60136 (59), the sequence of which was aligned with two related IncQ plasmids from *K. pneumoniae* (pKPC05 with 87.58% overall sequence identity and pB29 with 84.61% overall sequence identity) using Easyfig 2.2.5. Arrows represent genes as follows: β-lactamase encoding genes (green); replication-related genes (red); other genes of known function (orange); and genes of unknown function (blue). (B) A global phylogeny of class A β-lactamases was constructed by sequence comparison of class A β-lactamases from BLDB. The sequences displayed were retrieved from BLDB allowing for at least 40% sequence identity. The position of BKC-1 is denoted in bold. GPC-1, a β-lactamase identified in *P. aeruginosa*, showed the greatest amino acid sequence identity to BKC-1 (77%), while the next closest relationship (63% sequence identity) was with the chromosomally encoded β-lactamase (PAD-1) from *P. desertii*. The four rings that designate features in the phylogeny are as indicated in the legend.
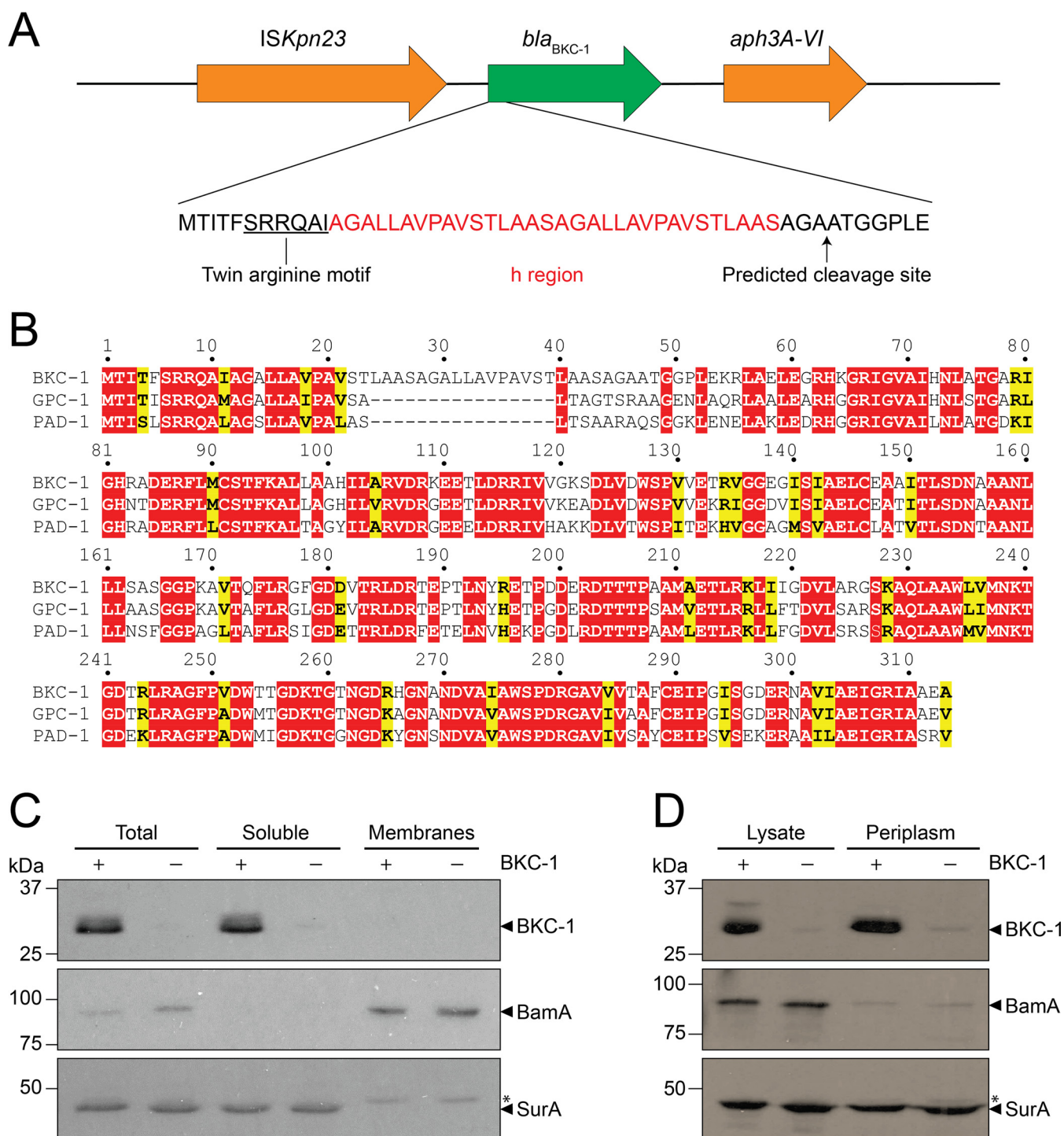
A

ISKpn23   bla_BKC-1   aph3A-VI

MTITF<u>SRRQAI</u>AGALLAVPAVSTLAASAGALLAVPAVSTLAASAGAATGGPLE

Twin arginine motif   h region   Predicted cleavage site

B

```
           1        10        20        30        40        50        60        70        80
BKC-1  MTITFSRRQAIAGALLAVPAVSTLAASAGALLAVPAVSTLAASAGAATGGPLEKRLAELEGRHKGRIGVAIHNLATGARI
GPC-1  MTITISRRQAMAGALLAIPAVSA----------------LTAGTSRAAGENLAQRLAALEARHGGRIGVAIHNLSTGARL
PAD-1  MTISLSRRQALAGSLLAVPALAS----------------LTSAARAQSGGKLENELAKLEDRHGGRIGVAILNLATGDKI

          81        90        100       110       120       130       140       150       160
BKC-1  GHRADERFLMCSTFKALLAAHILARVDRKEETLDRRIVGKSDLVDWSPVVETRVGGEGISIAELCEAAITLSDNAAANL
GPC-1  GHNTDERFLMCSTFKALLAGHILVRVDRGEETLDRRIVVKEADLVDWSPVVEKRIGGDVISIAELCEATITLSDNAAANL
PAD-1  GHRADERFLLCSTFKALTAGYILARVDRGEEELDRRIVHAKKDLVTWSPITEKHVGGAGMSVAELCLATVTLSDNTAANL

          161       170       180       190       200       210       220       230       240
BKC-1  LLSASGGPKAVTQFLRGFGDDVTRLDRTEPTLNYRETPDDERDTTTPAAMAETLRKLIIGDVLARGSKAQLAAWLVMNKT
GPC-1  LLAASGGPKAVTAFLRGLGDEVTRLDRTEPTLNYHETPGDERDTTTPSAMVETLRRLLFTDVLSARSKAQLAAWLIMNKT
PAD-1  LLNSFGGPAGLTAFLRSIGDETTRLDRFETELNVHEKPGDLRDTTTPAAMLETLRKLLFGDVLSRSSRAQLAAWMVMNKT

          241       250       260       270       280       290       300       310
BKC-1  GDTRLRAGFPVDWTTGDKTGTNGDRHGNANDVAIAWSPDRGAVVVTAFCEIPGISGDERNAVIAEIGRIAAEA
GPC-1  GDTRLRAGFPADWMTGDKTGTNGDKANANDVAVAWSPDRGAVIVAAFCEIPGISGDERNAVIAEIGRIAAEV
PAD-1  GDEKLRAGFPADWMIGDKTGGNGDKYGNSNDVAVAWSPDRGAVIVSAYCEIPSVSEKERAAILAEIGRIASRV
```

C

Total   Soluble   Membranes
kDa   +   −   +   −   +   −   BKC-1
37
25   ◄ BKC-1
100
75   ◄ BamA
50   * ◄ SurA

D

Lysate   Periplasm
kDa   +   −   +   −   BKC-1
37
25   ◄ BKC-1
100
75   ◄ BamA
50   * ◄ SurA

FIG 2 A unique signal sequence targets BKC-1 into the periplasm. (A) The position and sequence of the signal peptide encoded in bla_BKC-1. The twin arginine motif (underlined), 32-residue h-region (red), and cleavage site (AGA-AT) are indicated. (B) Protein sequence alignment of BKC-1 from *K. pneumoniae*, GPC-1 from *P. aeruginosa*, and PAD-1 from *P. desertii*. Red indicates identical residues; yellow indicates conserved residues. (C and D) Cell lysates from *E. coli* transformed with pJPCmR (−) or pJPBKC-1His encoding C-terminally His₆-tagged BKC-1 (+) were fractionated (C) or TSE-extracted (D) and analyzed by SDS-PAGE and immunoblotting using antibodies raised against BKC-1, BamA (membrane protein control), or SurA (periplasmic protein control). Asterisks indicate the slower-migrating nonspecific protein present in SurA immunoblots.

translocation. To determine whether BKC-1 activity in *E. coli* was similar to that seen in *K. pneumoniae*, the coding sequence of bla_BKC-1 was cloned under either a constitutive TetR promoter in pACYC184 (66) or a tetracycline-inducible promoter in pJPCmR (67). *K. pneumoniae* B5055 and *E. coli* BW25113 were transformed with each plasmid and antibiotic

TABLE 1 MIC assessment of *E. coli* BW25113 and *K. pneumoniae* B5055 expressing BKC-1

	MIC (µg/ml)										
	E. coli BW25113					*K. pneumoniae* B5055					
	No plasmid	Constitutive		Induced		No plasmid	Constitutive		Induced		Break point[a]
Drug		pACYC184	+BKC-1	pJPCmR	+BKC-1		pACYC184	+BKC-1	pJPCmR	+BKC-1	
Ampicillin	4	4	>1,024	4	>1,024	4	4	>1,024	4	>1,024	≥32
Ceftriaxone	≤0.0625	≤0.0625	64	≤0.0625	>64	≤0.0625	≤0.0625	64	≤0.0625	>64	≥4
Cefotaxime	≤0.0625	≤0.0625	64	≤0.0625	>64	≤0.0625	≤0.0625	32	≤0.0625	64	≥4
Ceftazidime	0.25	<0.25	4	0.25	8	0.25	0.25	8	0.25	8	≥16
Imipenem	0.125	0.125	2	0.125	4	0.5	0.5	4	0.5	4	≥4
Meropenem	0.03125	0.03125	1	0.03125	1	0.03125	0.03125	1	0.03125	1	≥4
Ertapenem	≤0.01<u>5</u>	≤0.015	0.5	≤0.015	0.5	≤0.015	≤0.015	1	≤0.015	1	≥2

[a]CLSI M100-ED30 breakpoint.

sensitivity was assessed by MIC assays. In addition to ampicillin, the broad-spectrum cephalosporin drugs ceftriaxone, ceftazidime, and cefotaxime were tested, as were the carbapenems imipenem, meropenem, and ertapenem. All BKC-1-expressing strains had similar levels of resistance toward each β-lactam tested (Table 1). The MIC values showed similar trends for both species regardless of whether the carbapenemase was under the control of a constitutive or inducible promoter. MICs for cells expressing BKC-1 were either at or below the breakpoint for resistance for all three carbapenems and ceftazidime (Table 1), while MICs for ampicillin, ceftriaxone, and cefotaxime were higher than the breakpoint, consistent with previous findings that BKC-1 does not hydrolyze carbapenems and ceftazidime as efficiently as other antibiotics tested (59). Growth curve analysis of *E. coli* BW25113 harboring plasmid-encoded BKC-1 showed that its expression did not impose a fitness cost (Fig. S2), whereas for *K. pneumoniae* B5055, a moderately lower growth rate was observed (Fig. S2).

To determine the localization of BKC-1 in *E. coli* BW25113, subcellular fractionation was undertaken using lysates prepared from cells expressing C-terminally hexahistidine (His$_6$)-tagged BKC-1 following 4 h of anhydrotetracycline (ATc) induction. Immunoblotting confirmed BKC-1 to be present exclusively in the soluble cellular fraction (combined cytoplasm and periplasm), and absent from membranes (Fig. 2C). This finding indicates that the unusually long signal sequence of BKC-1 is not acting as an inner membrane anchor. To confirm that the protein was periplasmic, osmotic shock was used to release the periplasmic contents and immunoblotting (Fig. 2D) confirmed BKC-1 to be localized to the periplasm.

Loss of TatC diminishes β-lactam resistance conferred by BKC-1. TatC is an essential component of the Tat system that interacts with substrate proteins via the twin arginine motif of the signal peptide (68). This binding step initiates the full assembly of the Tat translocon and subsequent transport of substrate across the inner membrane (50, 69). Sequence analysis suggested the signal peptide of BKC-1 has features consistent with the protein being a substrate of the Tat pathway (Table 2). To assess the role of the Tat system in β-lactamase translocation into the periplasm, C-terminally His$_6$-tagged BKC-1 was expressed in BW25113 and/or the isogenic $\Delta tatC$ mutant (70). As controls, the β-lactamases KPC-2 (putatively Sec dependent) and L2 (Tat dependent) were concomitantly expressed with a His$_6$ epitope incorporated at the C terminus of each protein. The expression of these β-lactamases did not compromise the growth of *E. coli* BW25113 nor its isogenic $\Delta tatC$ mutant (Fig. S3), except that L2 imposed minor fitness defects.

As a clinically relevant readout for enzymatically active β-lactamases, antibiotic sensitivity to ampicillin, three cephalosporins, and three carbapenems was assessed using MIC assays in the presence of anhydrotetracycline (ATc) (Table 3). Surprisingly, the phenotype of the $\Delta tatC$ mutant producing BKC-1 was drug dependent. In the case of ceftazidime, detectable resistance conferred by BKC-1 was strictly dependent on the

TABLE 2 Signal sequence analysis of BKC-1, BKC-1A, KPC-2, and L2

Protein	Signal sequence[b]	Tat probability score	Maximum S score[a]
BKC-1	MTITF**SRRQAI**AGALLAVPAVSTLAASAGALLAVPAVSTLAASAGA	0.84	0.843
BKC-1A	MTITF**SRRQAI**AGALLAVPAVSTLAASAGA	0.93	0.853
KPC-2	MSLYR**RL**VLLSCLSWPLAGFSATA	0.01	0.223
L2	MLA**RRRFLQ**FSGAAVASSLALPLLARAAGKATANA	0.99	0.841

[a]Score obtained from TatP 1.0 (cutoff 0.75).
[b]Twin arginine motifs are in boldface type and h regions are underlined.

presence of TatC (Table 3). However, resistance to cefotaxime, ampicillin, and ceftriaxone, although reduced in the ΔtatC mutant, was not completely abolished by inactivation of the Tat pathway (Table 3). MICs of ΔtatC mutant cells expressing BKC-1 were reduced by more than 2-fold for ampicillin, ceftriaxone, and cefotaxime, 32-fold for ceftazidime, and 2-fold for all three carbapenems tested. These observations suggest that the transport of BKC-1 is, at least in part, dependent on the Tat system; however, there is clearly some translocation of the enzyme in a Tat-independent manner.

The substrate-activity profile for BKC-1 revealed that the enzyme has marginal activity toward ceftazidime relative to the other β-lactam antibiotics tested (MIC of 8 μg/ml compared to at least 64 μg/ml for the other drugs shown in Table 3). This suggests that the decreased level of BKC-1 accumulating in the periplasm in the absence of TatC is likely sufficient to hydrolyze β-lactam drugs that are good substrates for the enzyme, but insufficient to turn over drugs such as ceftazidime, for which the enzyme is less well suited. As expected, KPC-2 activity as revealed through MIC values was unaffected in the ΔtatC mutant strain, confirming its translocation to be independent of the Tat system. In contrast, L2 activity was strictly dependent on TatC and the sensitivity of the ΔtatC mutants was 64-fold less, for all four drugs tested. This is consistent with previously findings that L2 is exclusively a substrate of the Tat translocon and its translocation does not rely on the Sec pathway (47).

To support these observations, immunoblotting was undertaken on whole-cell samples. Even following overexposure, the His$_6$-tagged epitope on L2 could not be detected in either wild-type or ΔtatC mutant backgrounds (Fig. 3A). This suggests that the tag may be proteolytically removed from this construct, since the protein is clearly present and functional, as judged by the phenotypes displayed in the MIC evaluation of these strains (Table 3). The level of KPC-2 expression appeared to be relatively similar in wild-type and ΔtatC mutant cells (Fig. 3A), also consistent with the phenotype observed from MIC experiments. In the tatC$^+$ background, BKC-1 appeared to be present at higher levels than KPC-2, and the vast majority of the protein was present as the processed, mature form (Fig. 3A). In contrast, in the ΔtatC mutant, although some tagged BKC-1 of the mature size was detected, a slower-migrating form of the protein

TABLE 3 MIC assessment of *E. coli* expressing BKC-1, KPC-2, and L2 in the presence and absence of TatC

	MIC (μg/ml)									
	BW25113					BW25113 ΔtatC				
		Induced					Induced			
Drug	No plasmid	pJPCmR	+BKC-1	+KPC-2	+L2	No plasmid	pJPCmR	+BKC-1	+KPC-2	+L2
Ampicillin	4	4	>1,024	>1,024	>1,024	4	4	512	>1,024	4
Ceftriaxone	≤0.0625	≤0.0625	>64	32	>64	≤0.0625	≤0.0625	64	32	≤0.0625
Cefotaxime	≤0.0625	≤0.0625	>64	16	64	≤0.0625	≤0.0625	32	16	≤0.0625
Ceftazidime	0.25	0.25	8	8	32	0.25	0.25	0.25	8	0.25
Imipenem	0.125	0.125	4	8	NT[a]	0.125	0.125	2	8	NT
Meropenem	0.03125	0.03125	1	4	NT	≤0.015	≤0.015	0.5	4	NT
Ertapenem	≤0.015	≤0.015	0.5	4	NT	≤0.015	≤0.015	0.25	4	NT

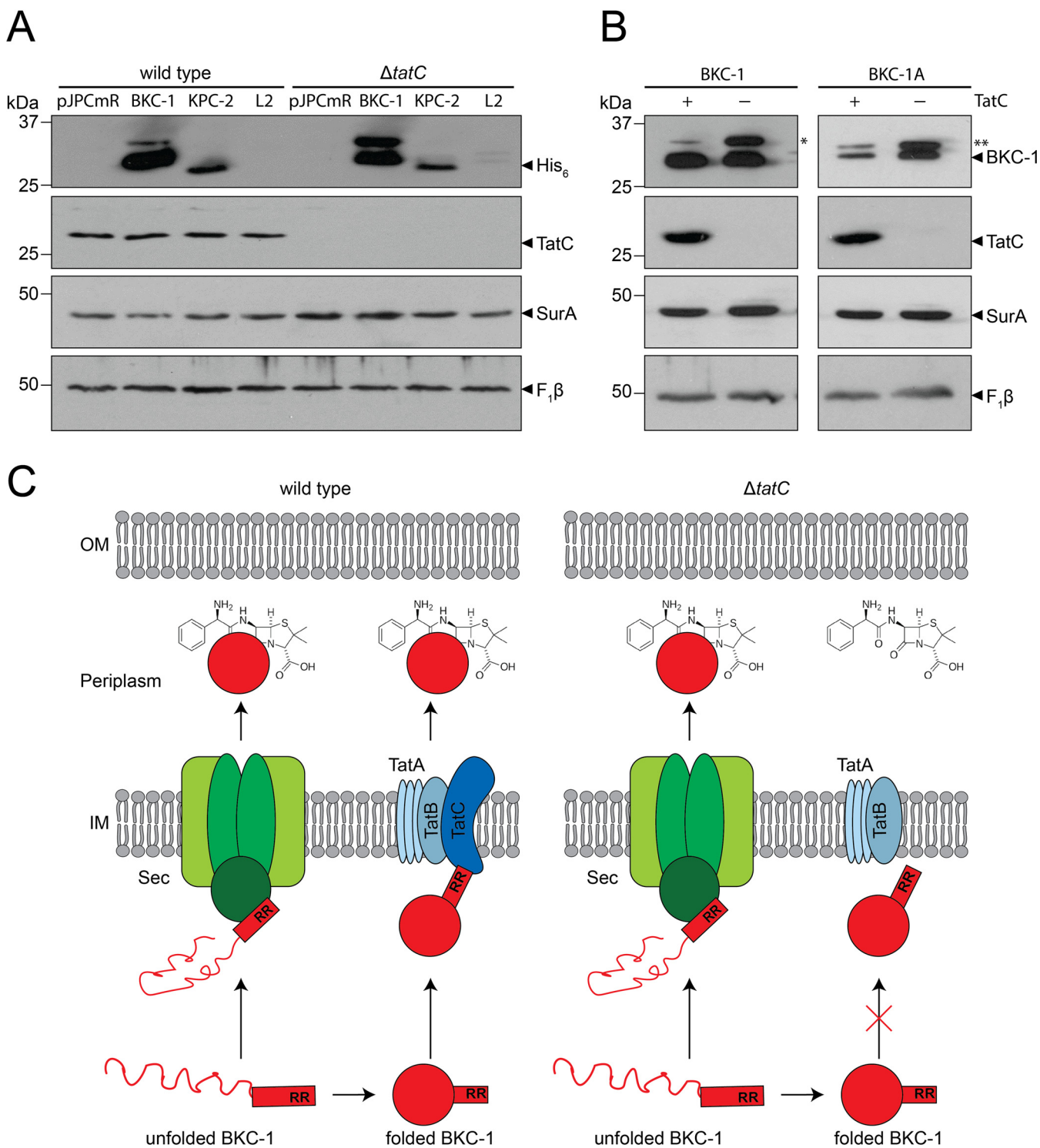[a]NT, not tested, because L2 is not a carbapenemase.

FIG 3 The unique signal sequence of BKC-1 is required for efficient Tat-independent translocation into the periplasm. (A and B) Whole-cell lysates were prepared from wild-type *E. coli* BW25113 or its isogenic Δ*tatC* mutant to compare levels of BKC-1 with other β-lactamases (A) or its BKC-1A derivative that has a shorter signal peptide (B). pJPCmR or its derivative vectors containing C-terminally His$_6$-tagged β-lactamases proteins were used to synthesize the indicated protein of interest (above immunoblot). The extracts were analyzed by SDS-PAGE and immunoblotting using antibodies raised against the indicated proteins (right of immunoblot). SurA and F$_1\beta$ serve as loading controls. Asterisks indicate precursor protein forms that migrate slower by SDS-PAGE. (C) The proposed model for the function and translocation of BKC-1 across the inner membrane (IM) in the presence and absence of TatC. The topological compartments of the periplasm and outer membrane (OM) are indicated. The unfolded and folded forms of BKC-1 (red) are shown and the rectangle with twin arginines (RR) represents its signal peptide. In the periplasm, both translocated forms of BKC-1 work together to hydrolyze β-lactam antibiotics, but in the absence of TatC, there is a decreased number of BKC-1 that can enter the periplasm.

TABLE 4 MIC assessment of *E. coli* expressing BKC-1 and BKC-1A in the presence and absence of TatC

Drug	MIC (μg/ml)							
	BW25113				BW25113 Δ*tatC*			
		Induced				Induced		
	No plasmid	pJPCmR	+BKC-1	+BKC-1A	No plasmid	pJPCmR	+BKC-1	+BKC-1A
Ampicillin	4	4	>1,024	>1,024	4	4	512	512
Ceftriaxone	≤0.0625	≤0.0625	>64	64	≤0.0625	≤0.0625	64	32
Cefotaxime	≤0.0625	≤0.0625	>64	64	≤0.0625	≤0.0625	32	16
Ceftazidime	0.25	0.25	8	2	0.25	0.25	0.25	0.25
Imipenem	0.125	0.125	4	2	0.125	0.125	2	1
Meropenem	0.03125	0.03125	1	0.5	≤0.015	≤0.015	0.5	0.25
Ertapenem	≤0.015	≤0.015	0.5	0.25	≤0.015	≤0.015	0.25	0.125

accumulated, at the expected size of the cytoplasmic unprocessed precursor. This is consistent with reduced translocation into the periplasm in the absence of a functional Tat pathway and is consistent with the reduced resistance phenotypes for ampicillin, ceftriaxone, and cefotaxime, as well as the Tat dependence seen for ceftazidime resistance (Table 3).

Signal peptide modification of BKC-1. The results presented above suggested that the targeting of BKC-1 is more complex than observed for other *β*-lactamases, being partially dependent on both Sec and Tat pathways. To address the extent to which the function of BKC-1 depends on its long signal sequence, we used GPC-1 and PAD-1 as models (Fig. 2B) to construct a modified sequence of BKC-1 (termed BKC-1A), where the 16-residue duplication of the h-region was removed. Expression of BKC-1A in *E. coli* BW25113 and its isogenic Δ*tatC* mutant imposed very minor fitness defects, similar to L2 expression (Fig. S3), but cell densities and growth rates were comparable to wild-type cells. We next assessed the phenotypic impact of truncating the BKC-1 signal peptide by measuring MICs using the same seven antibiotics as before in both the wild-type and the Δ*tatC* mutant background (Table 4). Although the 16-residue deletion did not affect resistance to ampicillin, the deletion did alter the resistances to all other drugs tested by at least 2-fold. MICs for cephalosporins with wild-type cells expressing BKC-1A were 2- to 4-fold lower than those expressing the native BKC-1 (Table 4). These effects were even more pronounced in the absence of TatC, where the MICs were 2-fold, 4-fold, and 8-fold lower for ceftriaxone, ceftazidime, and cefotaxime, respectively, compared to wild-type cells expressing BKC-1A. Carbapenem MICs were also 2-fold lower for cells expressing BKC-1A compared to those that expressed BKC-1 (Table 4), and this difference was preserved in the absence of TatC. Overall, this suggests that BKC-1 might be better suited for delivering a cephalosporin resistance phenotype than BKC-1A in the presence or absence of TatC.

To assess the relative levels of the carbapenemase in cells producing either BKC-1 or BKC-1A, immunoblotting was performed with whole-cell lysates using an antibody raised against BKC-1 (Fig. 3B). In each case, it appears there is more carbapenemase present in cells lacking TatC than in wild-type cells. For BKC-1, this increase in protein level does not appear to drastically affect the mature (periplasmic localized) form of the protein, but corresponds to an abundance of the precursor form of BKC-1. However, for BKC-1A, levels of precursor and mature forms of the protein are comparable, but there is a marked reduction in the amount of mature protein in the absence of a functional Tat translocon. Additionally, BKC-1A levels appeared to be lower than those of BKC-1 in the presence or absence of TatC (Fig. 3B). This is consistent with the MIC data (Table 4), where the expression of BKC-1 favors a more resistant phenotype than BKC-1A.

Assessing the importance of the twin arginine motif in BKC-1 in conferring resistance to *β*-lactams in *K. pneumoniae*. In order to determine whether the twin arginine motif was required for BKC-1 to confer a *β*-lactam resistant phenotype in *K.*

TABLE 5 MIC assessment of *K. pneumoniae* B5055 expressing BKC-1, BKC-1A and BKC-1KK

| Drug | MIC (µg/ml) | | | | |
| | No plasmid | Induced | | | |
		pJPCmR	+BKC-1	+BKC-1A	+BKC-1KK
Ampicillin	4	4	>1,024	>1,024	>1,024
Ceftriaxone	≤0.0625	≤0.0625	>64	>64	>64
Cefotaxime	≤0.0625	≤0.0625	64	64	32
Ceftazidime	0.25	0.25	8	2	0.25
Imipenem	0.5	0.5	4	2	4
Meropenem	0.03125	0.03125	1	1	1
Ertapenem	≤0.015	≤0.015	1	0.5	0.5

pneumoniae, the organism in which BKC-1 was discovered (59), we modified the signal peptide of BKC-1 by substituting the essential arginines for two lysines, a substitution known to abolish interaction with the Tat translocon (55, 69). Because we noted that BKC-1-dependent ceftazidime resistance in *E. coli* was dependent on a functional Tat translocon (Table 3 and 4), we assessed whether expression of this modified variant, BKC-1KK, in *K. pneumoniae* B5055 would similarly fail to confer resistance to ceftazidime. Indeed, the MIC measured in cells producing this variant was indistinguishable from cells lacking BKC-1 (MIC of 0.25 µg/ml; Table 5). While this signal peptide substitution prevents Tat translocation, it did not prevent BKC-1KK from being targeted to the Sec translocon because ampicillin resistance was not affected (MIC of >1,024 µg/ml; Table 5). We then assessed whether the 16-residue deletion in the signal peptide h-region (BKC-1A) would alter ceftazidime MICs in *K. pneumoniae*, and again found a 4-fold reduction (i.e., MIC of 2 µg/ml) compared to native BKC-1, similar to what was observed for *E. coli* (Table 4). Overall, this demonstrates that ceftazidime resistance conferred by BKC-1 is dependent on the Tat translocon in both *K. pneumoniae* and *E. coli*.

DISCUSSION

Theoretically, there are a number of restrictions to the dissemination of AMR and virulence phenotypes in bacteria by LGT (4, 5, 7). Our initial interest in BKC-1 was piqued by the observation that two related enzymes, BKC-1 and GPC-1, have each been identified only once and, despite being carried by highly transmissible plasmids, have not spread further by LGT or arisen more broadly than in the distinct countries where each was first found (59–61, 71). With only a few related sequences available, it is difficult to trace the exact origins of this lineage of carbapenemases, but a very recent report suggested that the plasmid-encoded BKC-1 may have originated from *Shinella*, given the oddity of its sequence (72). Whatever the ancestral reservoir for BKC-1 and related carbapenemases, genes transferred by LGT are often initially silenced by regulatory factors since they pose a potential risk to the host bacterium (1, 7, 73). It has been argued previously that one such risk to the host is that codon usage differences would impact on translation rates in these naive host species, or that protein translocation rates in cells expressing proteins acquired through LGT will block the biosynthetic machinery (74). Indeed, studies in *E. coli* showed that the overall assembly rates for virulence factors like FimD and UshC are dependent on how well features in these protein sequences can be handled by the components of the host cell's biosynthetic machinery (74). Similarly, for β-lactamases, a substantial fitness cost of carbapenem resistance has been quantified and linked to amino acid starvation due to codon usage incompatibility and other issues associated with maintaining sufficiently high expression levels of the carbapenemase (75).

For enzymes such as β-lactamases that function in the periplasm, translocation across the inner membrane can be achieved via either of two protein complexes, Sec

or Tat (39, 50). Here, the carbapenemase KPC-2 was found to engage with the Sec system for translocation into the periplasm, where it is presumably folded by periplasmic chaperones such as DsbA, which helps introduce disulfide bridges that are known to stabilize carbapenemases for optimum carbapenem hydrolysis (76), as is the paradigm for β-lactamase assembly reported in *Enterobacteriaceae* (47). Conversely, the Tat machinery translocates proteins folded in the cytoplasm, and L2 activity in the periplasm was shown to be wholly dependent on a functional Tat system, as reported previously (47). The increased sensitivity to β-lactams of *E. coli* harboring BKC-1 in the absence of TatC indicates that BKC-1 uses both translocation systems. Based on our findings, we suggest a dual-translocon targeting model for the export of BKC-1 (Fig. 3C). An interpretation of our data in terms of this model would be that BKC-1 is not yet especially adapted to either Sec or Tat in *Enterobacteriaceae*, but can deliver a highly β-lactam resistant phenotype only by using both arms of the host cell's protein translocation machinery. This implies that a subset of precursor BKC-1 remains unfolded in the cytoplasm (likely due to interactions with cytoplasmic chaperones), translocates via the Sec translocon, and later folds in the periplasm to assume its functional form, while the remaining subset of precursor BKC-1 folds in the cytoplasm, translocates via the Tat translocon, and assumes its functional form in the periplasm.

Experiments with BKC-1 and the truncated BKC-1A suggest that the extended signal peptide is advantageous in promoting the dual transport of BKC-1 to the periplasm. This was reflected as lower MICs of ceftriaxone, cefotaxime, and ceftazidime in cells expressing BKC-1A compared to those that expressed BKC-1 (Table 4). Given that this duplication was reported in BKC-1 obtained from *K. pneumoniae* isolates and is not present in its proposed ancestral counterparts (72), this feature may be an evolutionary snapshot of an adaptation optimizing BKC-1 phenotypes in *K. pneumoniae*. Inexplicably, under β-lactam selection in the laboratory, we observed a propensity for the signal peptide coding region of the gene encoding BKC-1 to undergo in-frame triple-nucleotide insertions (data not shown), suggesting a mechanism by which this region can enhance the compatibility between BKC-1 and the new host *E. coli*. It was also shown very recently that BKC-1 was able to hydrolyze ceftazidime in *E. coli*, better than its putative *Shinella* counterpart enzymes (72), perhaps suggesting that this duplication might have occurred under selection in the more closely related *Klebsiella*, thereby enhancing the activity of BKC-1 against ceftazidime. Given that BKC-1 activity against ceftazidime in *E. coli* was abolished in the absence of TatC (Table 3 and 4), and otherwise greatly reduced for the other cephalosporins tested in *E. coli*, we suspect that BKC-1 could have adapted its signal peptide to confer a stronger resistance phenotype against ceftazidime and related cephalosporins. The observation of a similar phenotype with *K. pneumoniae* cells expressing the variant of BKC-1 that avoids the Tat translocon (Table 5) further supports this possibility.

The concept of dual targeting as exemplified by BKC-1 is further supported by observations of LGT-induced translocon switching for β-lactamases. For example, the β-lactamase BlaC from *M. tuberculosis* is exclusively translocated via the Tat system (48). When BlaC is expressed in *E. coli*, its translocation into the periplasm is exclusively via the Sec translocon (47). This speaks to the requirement of cytoplasmic folding in *M. tuberculosis* and further suggests that this particular polypeptide is prevented from folding in the cytoplasm of *E. coli*. The exact mechanism underpinning the ability of BKC-1 to interact with components of both the Tat and Sec pathways and the evolution of its unique signal peptide remains unknown, and understanding the folding intermediates of this dual translocon targeting enzyme would warrant further studies.

In principle, the carbapenem-resistance phenotype is readily transmissible on plasmids via LGT. Outbreaks of CRE having been reported in various countries (77–81) and CRE (*K. pneumoniae*) have become endemic in various parts of the world (22, 79, 81–83). While LGT is usually considered in terms of its benefits for the recipient, the recipient bacteria also suffer fitness costs with plasmid carriage because of the burdens associated with acquisition and maintenance of large quantities of DNA, as well as the

need to correctly express, fold, and localize the "alien" proteins that these plasmids encode. In a given host scenario, the protein sequence features in a β-lactamase that increase protein folding efficiency do not necessarily correlate with enzyme efficiency and phenotype (84, 85), meaning the factors that drive the adaptability of β-lactamases in different species warrant further studies to better understand the spread of AMR phenotypes given current investments into next-generation antibiotics.

MATERIALS AND METHODS

Bacterial strains and plasmids. Strains and plasmids used in this study are listed in Table S1 and Table S2, respectively, in the supplemental material. Plasmid construction details are described in Text S1. Primers used in this study are listed in Table S3. All cultures were grown in LB with the appropriate antibiotics at 37°C, shaking at 200 rpm unless otherwise mentioned (2.5 cm orbit). Growth curves were performed as described previously (67).

Protein expression, extraction, and analysis. All strains containing pJPCmR and related vectors were grown to mid log-phase in LB supplemented with $34\,\mu$g/ml chloramphenicol and, if required, 35 ng/ml of anhydrotetracycline (ATc) for 4 h to induce protein expression. Crude cell lysates were prepared by harvesting 1 ml of cell culture and resuspending the pellets in an appropriate volume of SDS loading buffer (using a volume of 100 μl $\times$ the value of the optical density at 600 nm [OD_{600}]). Periplasmic protein extracts were prepared using Tris-sucrose-EDTA (TSE) as described previously (86). Protein fractionation was performed as described previously (87). BL21 Star (DE3) cells harboring pETBKC-1 to express soluble cytoplasmic C-terminally hexahistidine-tagged BKC-1 were grown to an OD_{600} of 0.4 at 37°C in terrific broth (1.2% wt/vol tryptone, 2.4% wt/vol yeast extract, 0.4% vol/vol glycerol, 17 mM KH_2PO_4, and 72 mM K_2HPO_4) supplemented with $100\,\mu$g/ml ampicillin. BKC-1 expression was induced by adding isopropyl-β-D-thiogalactopyranoside (IPTG) to a final concentration of 0.2 mM and growing the culture for 4 h at 37°C. Cell lysis, protein extraction, purification, and quantification were performed as described previously (88). Using this protein, rabbit polyclonal antibodies against BKC-1 were obtained. SDS-PAGE and immunoblotting were performed as described previously (89) using the antibodies listed in Table S4.

Antibiotic sensitivity assays. Cultures were grown to an OD_{600} of 0.6 to 0.7 and MICs were determined and analyzed using the broth microdilution method as outlined by CLSI (90). For cells that contained pJPCmR and its derivatives, cultures were grown to an OD_{600} of 0.3 to 0.4 and then induced with ATc at a final concentration of 35 ng/ml until an OD_{600} of 0.6 to 0.7 was reached before performing MIC assays in the continued presence of ATc.

Sequence analysis. Plasmid DNA comparison was performed using Easyfig 2.2.5 (91). Sequences of BKC-1 and other β-lactamases were obtained from BLDB (63). The sequence of BKC-1 was used as a query sequence to probe the database using the inbuilt BLDB BLAST function, and the top 200 hits were collected after setting a 40% sequence identity cutoff. Phylogeny trees were visualized using iTOL v4 (64) from alignments generated using Clustal Omega (92). Signal peptide analysis of BKC-1, BKC-1A, KPC-2, and L2 was performed using TatP 1.0 (93) and SignalP 5.0 (94) and all sequence alignments were visualized using ESPript (95).

SUPPLEMENTAL MATERIAL

Supplemental material is available online only.

TEXT S1, DOCX file, 0.01 MB.
FIG S1, PDF file, 1.1 MB.
FIG S2, PDF file, 0.7 MB.
FIG S3, PDF file, 0.7 MB.
TABLE S1, PDF file, 0.2 MB.
TABLE S2, PDF file, 0.2 MB.
TABLE S3, PDF file, 0.1 MB.
TABLE S4, PDF file, 0.1 MB.
TABLE S5, PDF file, 0.5 MB.

REFERENCES

1. Tuller T, Girshovich Y, Sella Y, Kreimer A, Freilich S, Kupiec M, Gophna U, Ruppin E. 2011. Association between translation efficiency and horizontal gene transfer within microbial communities. Nucleic Acids Res 39:4743–4755. https://doi.org/10.1093/nar/gkr054.

2. Dalbey RE, Kuhn A. 2012. Protein traffic in Gram-negative bacteria—how exported and secreted proteins find their way. FEMS Microbiol Rev 36:1023–1045. https://doi.org/10.1111/j.1574-6976.2012.00327.x.

3. Bogumil D, Dagan T. 2012. Cumulative impact of chaperone-mediated folding on genome evolution. Biochemistry 51:9941–9953. https://doi.org/10.1021/bi3013643.

4. Ochman H, Lawrence JG, Groisman EA. 2000. Lateral gene transfer and the nature of bacterial innovation. Nature 405:299–304. https://doi.org/10.1038/35012500.

5. Ruzzini AC, Clardy J. 2016. Gene flow and molecular innovation in bacteria. Curr Biol 26:R859–R864. https://doi.org/10.1016/j.cub.2016.08.004.

6. Boto L. 2015. Horizontal gene transfer in evolution. eLS 1–7. John Wiley & Sons, Ltd, Chichester, UK. https://doi.org/10.1002/9780470015902.a0022835.pub2.

7. Thomas CM, Nielsen KM. 2005. Mechanisms of, and barriers to, horizontal gene transfer between bacteria. Nat Rev Microbiol 3:711–721. https://doi.org/10.1038/nrmicro1234.

8. Ventola CL. 2015. The antibiotic resistance crisis: part 1: causes and threats. P T 40:277–283.

9. Nikaido H. 2009. Multidrug resistance in bacteria. Annu Rev Biochem 78:119–146. https://doi.org/10.1146/annurev.biochem.78.082907.145923.

10. Bush K. 2018. Past and present perspectives on β-lactamases. Antimicrob Agents Chemother 62:e01076-18. https://doi.org/10.1128/AAC.01076-18.

11. Bush K. 2010. Bench-to-bedside review: the role of β-lactamases in antibiotic-resistant Gram-negative infections. Crit Care 14:224. https://doi.org/10.1186/cc8892.

12. Codjoe FS, Donkor ES. 2017. Carbapenem resistance: a review. Med Sci 6:1. https://doi.org/10.3390/medsci6010001.

13. Bush K, Bradford PA. 2016. β-Lactams and β-lactamase inhibitors: an overview. Cold Spring Harb Perspect Med 6:a025247. https://doi.org/10.1101/cshperspect.a025247.

14. Suay-García B, Pérez-Gracia MT. 2019. Present and future of carbapenem-resistant Enterobacteriaceae (CRE) infections. Antibiotics (Basel) 8:122. https://doi.org/10.3390/antibiotics8030122.

15. Mathers AJ, Peirano G, Pitout JD. 2015. The role of epidemic resistance plasmids and international high-risk clones in the spread of multidrug-resistant Enterobacteriaceae. Clin Microbiol Rev 28:565–591. https://doi.org/10.1128/CMR.00116-14.

16. Rapp RP, Urban C. 2012. Klebsiella pneumoniae carbapenemases in Enterobacteriaceae: history, evolution, and microbiology concerns. Pharmacotherapy 32:399–407. https://doi.org/10.1002/j.1875-9114.2012.01035.x.

17. Yigit H, Queenan AM, Anderson GJ, Domenech-Sanchez A, Biddle JW, Steward CD, Alberti S, Bush K, Tenover FC. 2001. Novel carbapenem-hydrolyzing β-lactamase, KPC-1, from a carbapenem-resistant strain of Klebsiella pneumoniae. Antimicrob Agents Chemother 45:1151–1161. https://doi.org/10.1128/AAC.45.4.1151-1161.2001.

18. Arnold RS, Thom KA, Sharma S, Phillips M, Kristie Johnson J, Morgan DJ. 2011. Emergence of Klebsiella pneumoniae carbapenemase-producing bacteria. South Med J 104:40–45. https://doi.org/10.1097/SMJ.0b013e3181fd7d5a.

19. Mehta SC, Rice K, Palzkill T. 2015. Natural variants of the KPC-2 carbapenemase have evolved increased catalytic efficiency for ceftazidime hydrolysis at the cost of enzyme stability. PLoS Pathog 11:e1004949. https://doi.org/10.1371/journal.ppat.1004949.

20. Walther-Rasmussen J, Høiby N. 2007. Class A carbapenemases. J Antimicrob Chemother 60:470–482. https://doi.org/10.1093/jac/dkm226.

21. Wyres KL, Wick RR, Judd LM, Froumine R, Tokolyi A, Gorrie CL, Lam MMC, Duchêne S, Jenney A, Holt KE. 2019. Distinct evolutionary dynamics of horizontal gene transfer in drug resistant and virulent clones of Klebsiella pneumoniae. PLoS Genet 15:e1008114. https://doi.org/10.1371/journal.pgen.1008114.

22. Lee CR, Lee JH, Park KS, Kim YB, Jeong BC, Lee SH. 2016. Global dissemination of carbapenemase-producing Klebsiella pneumoniae: epidemiology, genetic context, treatment options, and detection methods. Front Microbiol 7:895. https://doi.org/10.3389/fmicb.2016.00895.

23. Ramirez MS, Xie G, Traglia GM, Johnson SL, Davenport KW, van Duin D, Ramazani A, Perez F, Jacobs MR, Sherratt DJ, Bonomo RA, Chain PS, Tolmasky ME. 2016. Whole-genome comparative analysis of two carbapenem-resistant ST-258 Klebsiella pneumoniae strains isolated during a north-eastern Ohio outbreak: differences within the high heterogeneity zones. Genome Biol Evol 8:2036–2043. https://doi.org/10.1093/gbe/evw135.

24. Hu YY, Cai JC, Zhou HW, Chi D, Zhang XF, Chen WL, Zhang R, Chen GX. 2013. Molecular typing of CTX-M-producing Escherichia coli isolates from environmental water, swine feces, specimens from healthy humans, and human patients. Appl Environ Microbiol 79:5988–5996. https://doi.org/10.1128/AEM.01740-13.

25. Isgren CM, Edwards T, Pinchbeck GL, Winward E, Adams ER, Norton P, Timofte D, Maddox TW, Clegg PD, Williams NJ. 2019. Emergence of carriage of CTX-M-15 in faecal Escherichia coli in horses at an equine hospital in the UK; increasing prevalence over a decade (2008–2017.). BMC Vet Res 15:268. https://doi.org/10.1186/s12917-019-2011-9.

26. Dehshiri M, Khoramrooz SS, Zoladl M, Khosravani SA, Parhizgari N, Motazedian MH, Jahedi S, Sharifi A. 2018. The frequency of Klebsiella pneumonia encoding genes for CTX-M, TEM-1 and SHV-1 extended-spectrum beta lactamases enzymes isolated from urinary tract infection. Ann Clin Microbiol Antimicrob 17:4. https://doi.org/10.1186/s12941-018-0256-y.

27. An S, Chen J, Wang Z, Wang X, Yan X, Li J, Chen Y, Wang Q, Xu X, Li J, Yang J, Wang H, Gao Z. 2012. Predominant characteristics of CTX-M-producing Klebsiella pneumoniae isolates from patients with lower respiratory tract infection in multiple medical centers in China. FEMS Microbiol Lett 332:137–145. https://doi.org/10.1111/j.1574-6968.2012.02586.x.

28. Cantón R, González-Alba JM, Galán JC. 2012. CTX-M enzymes: origin and diffusion. Front Microbiol 3:110. https://doi.org/10.3389/fmicb.2012.00110.

29. Bevan ER, Jones AM, Hawkey PM. 2017. Global epidemiology of CTX-M β-lactamases: temporal and geographical shifts in genotype. J Antimicrob Chemother 72:2145–2155. https://doi.org/10.1093/jac/dkx146.

30. Picão RC, Poirel L, Gales AC, Nordmann P. 2009. Further identification of CTX-M-2 extended-spectrum β-lactamase in Pseudomonas aeruginosa. Antimicrob Agents Chemother 53:2225–2226. https://doi.org/10.1128/AAC.01602-08.

31. Ogbolu DO, Alli OAT, Webber MA, Oluremi AS, Oloyede OM. 2018. CTX-M-15 is established in most multidrug-resistant uropathogenic Enterobacteriaceae and Pseudomonaceae from hospitals in Nigeria. Eur J Microbiol Immunol (Bp) 8:20–24. https://doi.org/10.1556/1886.2017.00012.

32. Laminet AA, Kumamoto CA, Plückthun A. 1991. Folding in vitro and transport in vivo of pre-β-lactamase are SecB independent. Mol Microbiol 5:117–122. https://doi.org/10.1111/j.1365-2958.1991.tb01832.x.

33. Beha D, Deitermann S, Müller M, Koch HG. 2003. Export of β-lactamase is independent of the signal recognition particle. J Biol Chem 278:22161–22167. https://doi.org/10.1074/jbc.M300929200.

34. Minsky A, Summers RG, Knowles JR. 1986. Secretion of β-lactamase into the periplasm of Escherichia coli: evidence for a distinct release step associated with a conformational change. Proc Natl Acad Sci U S A 83:4180–4184. https://doi.org/10.1073/pnas.83.12.4180.

35. Goemans C, Denoncin K, Collet JF. 2014. Folding mechanisms of periplasmic proteins. Biochim Biophys Acta 1843:1517–1528. https://doi.org/10.1016/j.bbamcr.2013.10.014.

36. Miot M, Betton JM. 2004. Protein quality control in the bacterial periplasm. Microb Cell Fact 3:4. https://doi.org/10.1186/1475-2859-3-4.

37. Chum AP, Shoemaker SR, Fleming PJ, Fleming KG. 2019. Plasticity and transient binding are key ingredients of the periplasmic chaperone network. Protein Sci 28:1340–1349. https://doi.org/10.1002/pro.3641.

38. Costello SM, Plummer AM, Fleming PJ, Fleming KG. 2016. Dynamic periplasmic chaperone reservoir facilitates biogenesis of outer membrane proteins. Proc Natl Acad Sci U S A 113:E4794–800. https://doi.org/10.1073/pnas.1601002113.

39. Tsirigotaki A, De Geyter J, Šoštaric N, Economou A, Karamanou S. 2017. Protein export through the bacterial Sec pathway. Nat Rev Microbiol 15:21–36. https://doi.org/10.1038/nrmicro.2016.161.

40. Rusch SL, Kendall DA. 2007. Interactions that drive Sec-dependent bacterial protein transport. Biochemistry 46:9665–9673. https://doi.org/10.1021/bi7010064.

41. Suvorov M, Vakulenko SB, Mobashery S. 2007. Cytoplasmic-membrane anchoring of a class A β-lactamase and its capacity in manifesting antibiotic resistance. Antimicrob Agents Chemother 51:2937–2942. https://doi.org/10.1128/AAC.00011-07.

42. Massova I, Mobashery S. 1998. Kinship and diversification of bacterial penicillin-binding proteins and β-lactamases. Antimicrob Agents Chemother 42:1–17. https://doi.org/10.1128/AAC.42.1.1.

43. de Sousa Borges A, de Keyzer J, Driessen AJ, Scheffers DJ. 2015. The Escherichia coli membrane protein insertase YidC assists in the biogenesis of

penicillin binding proteins. J Bacteriol 197:1444–1450. https://doi.org/10.1128/JB.02556-14.

44. Bradford PA. 2001. Extended-spectrum β-lactamases in the 21st century: characterization, epidemiology, and detection of this important resistance threat. Clin Microbiol Rev 14:933–951. https://doi.org/10.1128/CMR.14.4.933-951.2001.

45. Pascual V, Ortiz G, Simó M, Alonso N, Garcia MC, Xercavins M, Rivera A, Morera MA, Miró E, Espejo E, Navarro F, Gurguí M, Pérez J, Rodríguez-Carballeira M, Garau J, Calbo E. 2015. Epidemiology and risk factors for infections due to AmpC β-lactamase-producing Escherichia coli. J Antimicrob Chemother 70:899–904. https://doi.org/10.1093/jac/dku468.

46. Pai H, Kang CI, Byeon JH, Lee KD, Park WB, Kim HB, Kim EC, Oh MD, Choe KW. 2004. Epidemiology and clinical features of bloodstream infections caused by AmpC-type-β-lactamase-producing Klebsiella pneumoniae. Antimicrob Agents Chemother 48:3720–3728. https://doi.org/10.1128/AAC.48.10.3720-3728.2004.

47. Pradel N, Delmas J, Wu LF, Santini CL, Bonnet R. 2009. Sec- and Tat-dependent translocation of β-lactamases across the Escherichia coli inner membrane. Antimicrob Agents Chemother 53:242–248. https://doi.org/10.1128/AAC.00642-08.

48. McDonough JA, Hacker KE, Flores AR, Pavelka MS, Jr., Braunstein M. 2005. The twin-arginine translocation pathway of Mycobacterium smegmatis is functional and required for the export of mycobacterial beta-lactamases. J Bacteriol 187:7667–7679. https://doi.org/10.1128/JB.187.22.7667-7679.2005.

49. Palmer T, Stansfeld PJ. 2020. Targeting of proteins to the twin-arginine translocation pathway. Mol Microbiol 113:861–871. https://doi.org/10.1111/mmi.14461.

50. Palmer T, Berks BC. 2012. The twin-arginine translocation (Tat) protein export pathway. Nat Rev Microbiol 10:483–496. https://doi.org/10.1038/nrmicro2814.

51. Stanley NR, Palmer T, Berks BC. 2000. The twin arginine consensus motif of Tat signal peptides is involved in Sec-independent protein targeting in Escherichia coli. J Biol Chem 275:11591–11596. https://doi.org/10.1074/jbc.275.16.11591.

52. Bogsch E, Brink S, Robinson C. 1997. Pathway specificity for a ΔpH-dependent precursor thylakoid lumen protein is governed by a 'Sec-avoidance' motif in the transfer peptide and a 'Sec-incompatible' mature protein. EMBO J 16:3851–3859. https://doi.org/10.1093/emboj/16.13.3851.

53. Tooke FJ, Babot M, Chandra G, Buchanan G, Palmer T. 2017. A unifying mechanism for the biogenesis of membrane proteins co-operatively integrated by the Sec and Tat pathways. Elife 6:e26577. https://doi.org/10.7554/eLife.26577.

54. Tullman-Ercek D, DeLisa MP, Kawarasaki Y, Iranpour P, Ribnicky B, Palmer T, Georgiou G. 2007. Export pathway selectivity of Escherichia coli twin arginine translocation signal peptides. J Biol Chem 282:8309–8316. https://doi.org/10.1074/jbc.M610507200.

55. Huang Q, Palmer T. 2017. Signal peptide hydrophobicity modulates interaction with the twin-arginine translocase. mBio 8:e00909-17. https://doi.org/10.1128/mBio.00909-17.

56. Berks BC. 2015. The twin-arginine protein translocation pathway. Annu Rev Biochem 84:843–864. https://doi.org/10.1146/annurev-biochem-060614-034251.

57. Hamsanathan S, Musser SM. 2018. The Tat protein transport system: intriguing questions and conundrums. FEMS Microbiol Lett 365:fny123. https://doi.org/10.1093/femsle/fny123.

58. Kouwen TR, van der Ploeg R, Antelmann H, Hecker M, Homuth G, Mäder U, van Dijl JM. 2009. Overflow of a hyper-produced secretory protein from the Bacillus Sec pathway into the Tat pathway for protein secretion as revealed by proteogenomics. Proteomics 9:1018–1032. https://doi.org/10.1002/pmic.200800580.

59. Nicoletti AG, Marcondes MF, Martins WM, Almeida LG, Nicolás MF, Vasconcelos AT, Oliveira V, Gales AC. 2015. Characterization of BKC-1 class A carbapenemase from Klebsiella pneumoniae clinical isolates in Brazil. Antimicrob Agents Chemother 59:5159–5164. https://doi.org/10.1128/AAC.00158-15.

60. Lv R, Guo J, Yan Y, Chen R, Xiao L, Wang M, Fang N, Fang C, Cui Y, Yang R, Song Y. 2017. Characterization of a novel class A carbapenemase PAD-1 from Paramesorhizobium desertii A-3-E(T), a strain highly resistant to β-lactam antibiotics. Sci Rep 7:8370. https://doi.org/10.1038/s41598-017-07841-1.

61. Schauer J, Gatermann SG, Hoffmann D, Hupfeld L, Pfennigwerth N. 2020. GPC-1, a novel class A carbapenemase detected in a clinical Pseudomonas aeruginosa isolate. J Antimicrob Chemother 75:911–916. https://doi.org/10.1093/jac/dkz536.

62. Cuzon G, Naas T, Nordmann P. 2011. Functional characterization of Tn4401, a Tn3-based transposon involved in bla_KPC gene mobilization. Antimicrob Agents Chemother 55:5370–5373. https://doi.org/10.1128/AAC.05202-11.

63. Naas T, Oueslati S, Bonnin RA, Dabos ML, Zavala A, Dortet L, Retailleau P, Iorga BI. 2017. Beta-lactamase database (BLDB)—structure and function. J Enzyme Inhib Med Chem 32:917–919. https://doi.org/10.1080/14756366.2017.1344235.

64. Letunic I, Bork P. 2019. Interactive tree of life (iTOL) v4: recent updates and new developments. Nucleic Acids Res 47:W256–W259. https://doi.org/10.1093/nar/gkz239.

65. Payne SH, Bonissone S, Wu S, Brown RN, Ivankov DN, Frishman D, Pasa-Tolić L, Smith RD, Pevzner PA. 2012. Unexpected diversity of signal peptides in prokaryotes. mBio 3:e00339-12. https://doi.org/10.1128/mBio.00339-12.

66. Chang AC, Cohen SN. 1978. Construction and characterization of amplifiable multicopy DNA cloning vehicles derived from the P15A cryptic miniplasmid. J Bacteriol 134:1141–1156. https://doi.org/10.1128/JB.134.3.1141-1156.1978.

67. Rocker A, Lacey JA, Belousoff MJ, Wilksch JJ, Strugnell RA, Davies MR, Lithgow T. 2020. Global trends in proteome remodeling of the outer membrane modulate antimicrobial permeability in Klebsiella pneumoniae. mBio 11:e00603-20. https://doi.org/10.1128/mBio.00603-20.

68. Rollauer SE, Tarry MJ, Graham JE, Jääskeläinen M, Jäger F, Johnson S, Krehenbrink M, Liu SM, Lukey MJ, Marcoux J, McDowell MA, Rodriguez F, Roversi P, Stansfeld PJ, Robinson CV, Sansom MS, Palmer T, Högbom M, Berks BC, Lea SM. 2012. Structure of the TatC core of the twin-arginine protein transport system. Nature 492:210–214. https://doi.org/10.1038/nature11683.

69. Alami M, Lüke I, Deitermann S, Eisner G, Koch HG, Brunner J, Müller M. 2003. Differential interactions between a twin-arginine signal peptide and its translocase in Escherichia coli. Mol Cell 12:937–946. https://doi.org/10.1016/s1097-2765(03)00398-8.

70. Baba T, Ara T, Hasegawa M, Takai Y, Okumura Y, Baba M, Datsenko KA, Tomita M, Wanner BL, Mori H. 2006. Construction of Escherichia coli K-12 in-frame, single-gene knockout mutants: the Keio collection. Mol Syst Biol 2:2006. https://doi.org/10.1038/msb4100050.

71. Martins WM, Nicoletti AG, Santos SR, Sampaio JL, Gales AC. 2016. Frequency of BKC-1-producing Klebsiella species isolates. Antimicrob Agents Chemother 60:5044–5046. https://doi.org/10.1128/AAC.00470-16.

72. Kieffer N, Ebmeyer S, Larsson DGJ. 2020. The class a carbapenemases BKC-1 and GPC-1 both originate from the bacterial genus Shinella. Antimicrob Agents Chemother 64:e01263-20. https://doi.org/10.1128/AAC.01263-20.

73. Lucchini S, Rowley G, Goldberg MD, Hurd D, Harrison M, Hinton JC. 2006. H-NS mediates the silencing of laterally acquired genes in bacteria. PLoS Pathog 2:e81. https://doi.org/10.1371/journal.ppat.0020081.

74. Stubenrauch CJ, Dougan G, Lithgow T, Heinz E. 2017. Constraints on lateral gene transfer in promoting fimbrial usher protein diversity and function. Open Biol 7:170144. https://doi.org/10.1098/rsob.170144.

75. Cheung CHP, Alorabi M, Hamilton F, Takebayashi Y, Mounsey O, Heesom KJ, Williams PB, Williams OM, Albur M, MacGowan AP, Avison MB. 2020. Trade-offs between antibacterial resistance and fitness cost in the production of metallo-β-lactamase by enteric bacteria manifest as sporadic emergence of carbapenem resistance in a clinical setting. bioRxiv https://doi.org/10.1101/2020.10.24.353581:2020.10.24.353581.

76. Smith CA, Nossoni Z, Toth M, Stewart NK, Frase H, Vakulenko SB. 2016. Role of the conserved disulfide bridge in Class A carbapenemases. J Biol Chem 291:22196–22206. https://doi.org/10.1074/jbc.M116.749648.

77. Palmore TN, Henderson DK. 2013. Managing transmission of carbapenem-resistant Enterobacteriaceae in healthcare settings: a view from the trenches. Clin Infect Dis 57:1593–1599. https://doi.org/10.1093/cid/cit531.

78. Schwaber MJ, Klarfeld-Lidji S, Navon-Venezia S, Schwartz D, Leavitt A, Carmeli Y. 2008. Predictors of carbapenem-resistant Klebsiella pneumoniae acquisition among hospitalized adults and effect of acquisition on mortality. AAC 52:1028–1033. https://doi.org/10.1128/AAC.01020-07.

79. Souli M, Galani I, Antoniadou A, Papadomichelakis E, Poulakou G, Panagea T, Vourli S, Zerva L, Armaganidis A, Kanellakopoulou K, Giamarellou H. 2010. An outbreak of infection due to beta-lactamase Klebsiella pneumoniae carbapenemase 2-producing K. pneumoniae in a Greek University Hospital: molecular characterization, epidemiology, and outcomes. Clin Infect Dis 50:364–373. https://doi.org/10.1086/649865.

80. Balm MN, Ngan G, Jureen R, Lin RT, Teo J. 2012. Molecular characterization of newly emerged bla_{KPC-2}-producing *Klebsiella pneumoniae* in Singapore. J Clin Microbiol 50:475–476. https://doi.org/10.1128/JCM.05914-11.

81. Sampaio JL, Gales AC. 2016. Antimicrobial resistance in *Enterobacteriaceae* in Brazil: focus on β-lactams and polymyxins. Braz J Microbiol 47 Suppl 1:31–37. https://doi.org/10.1016/j.bjm.2016.10.002.

82. Chang LW, Buising KL, Jeremiah CJ, Cronin K, Poy Lorenzo YS, Howden BP, Kwong J, Cocks J, Blood A, Greenough J, Waters MJ. 2015. Managing a nosocomial outbreak of carbapenem-resistant *Klebsiella pneumoniae*: an early Australian hospital experience. Intern Med J 45:1037–1043. https://doi.org/10.1111/imj.12863.

83. Xu G, Jiang Y, An W, Wang H, Zhang X. 2015. Emergence of KPC-2-producing *Escherichia coli* isolates in an urban river in Harbin, China. World J Microbiol Biotechnol 31:1443–1450. https://doi.org/10.1007/s11274-015-1897-z.

84. Wang X, Minasov G, Shoichet BK. 2002. Evolution of an antibiotic resistance enzyme constrained by stability and activity trade-offs. J Mol Biol 320:85–95. https://doi.org/10.1016/S0022-2836(02)00400-X.

85. Klesmith JR, Bacik JP, Wrenbeck EE, Michalczyk R, Whitehead TA. 2017. Trade-offs between enzyme fitness and solubility illuminated by deep mutational scanning. Proc Natl Acad Sci U S A 114:2265–2270. https://doi.org/10.1073/pnas.1614437114.

86. Hiniker A, Bardwell JC. 2004. *In vivo* substrate specificity of periplasmic disulfide oxidoreductases. J Biol Chem 279:12967–12973. https://doi.org/10.1074/jbc.M311391200.

87. Dunstan RA, Hay ID, Lithgow T. 2017. Defining membrane protein localization by isopycnic density gradients. Methods Mol Biol 1615:81–86. https://doi.org/10.1007/978-1-4939-7033-9_6.

88. Hardy JM, Dunstan RA, Grinter R, Belousoff MJ, Wang J, Pickard D, Venugopal H, Dougan G, Lithgow T, Coulibaly F. 2020. The architecture and stabilisation of flagellotropic tailed bacteriophages. Nat Commun 11:3748. https://doi.org/10.1038/s41467-020-17505-w.

89. Webb CT, Selkrig J, Perry AJ, Noinaj N, Buchanan SK, Lithgow T. 2012. Dynamic association of BAM complex modules includes surface exposure of the lipoprotein BamC. J Mol Biol 422:545–555. https://doi.org/10.1016/j.jmb.2012.05.035.

90. Clinical and Laboratory Standards Institute. 2012. Methods for dilution antimicrobial susceptibility tests for bacteria that grow aerobically, 9th ed. Clinical and Laboratory Standards Institute, Wayne, PA.

91. Sullivan MJ, Petty NK, Beatson SA. 2011. Easyfig: a genome comparison visualizer. Bioinformatics 27:1009–1010. https://doi.org/10.1093/bioinformatics/btr039.

92. Sievers F, Wilm A, Dineen D, Gibson TJ, Karplus K, Li W, Lopez R, McWilliam H, Remmert M, Söding J, Thompson JD, Higgins DG. 2011. Fast, scalable generation of high-quality protein multiple sequence alignments using Clustal Omega. Mol Syst Biol 7:539. https://doi.org/10.1038/msb.2011.75.

93. Bendtsen JD, Nielsen H, Widdick D, Palmer T, Brunak S. 2005. Prediction of twin-arginine signal peptides. BMC Bioinformatics 6:167. https://doi.org/10.1186/1471-2105-6-167.

94. Almagro Armenteros JJ, Tsirigos KD, Sønderby CK, Petersen TN, Winther O, Brunak S, von Heijne G, Nielsen H. 2019. SignalP 5.0 improves signal peptide predictions using deep neural networks. Nat Biotechnol 37:420–423. https://doi.org/10.1038/s41587-019-0036-z.

95. Robert X, Gouet P. 2014. Deciphering key features in protein structures with the new ENDscript server. Nucleic Acids Res 42:W320–4. https://doi.org/10.1093/nar/gku316.